Understanding coating strength at the molecular and microscopic level

MARTTI TOIVAKKA, PARVEZ ALAM, FARID TOUAITI, ANNIINA ORAVILAHTI, TUOMAS ORAVILAHTI, JUHA KNUUTINEN, ROBERT NILSSON, MAHDI PAHLEVAN, MIA AHOKAS, AND CARL-ERIC WILEN

ABSTRACT: Insufficient coating strength can lead to various problems in printing and converting of pigment-coated paper and paperboard. The loss in strength, especially in the presence of printing liquids, can result from poor adhesion between the binder and the coating pigments. Experiments and numerical simulations were used to better understand the microscopic and molecular level interactions between the latex-binder and dispersant-covered coating pigments used in paper coating. Micromechanical simulations were carried out to identify the microstructural variables most influential to strength. Several new pigment dispersing agents were synthesized with the reversible addition-fragmentation chain transfer copolymerization technique, and their dispersing effect and influence on dry and wet strength of pigment coating were evaluated. Molecular level interactions between binders, coating pigments, and various functional groups used in the dispersants were studied with molecular modeling. Furthermore, dynamic mechanical thermal analysis was used to examine the influence of both commercial and novel dispersants on the pigment-latex interactions. Some of the novel dispersants synthesized and tested show promise in improving the wet strength of the coating while providing as good as or better dispersing effect when compared to a sodium polyacrylate–based commercial dispersant.

Application: Mills that understand the interfacial phenomena of paper coatings at the molecular level can improve surface strength of pigment-coated paper and board and realize higher production cost efficiency.

While the increase in production of paper and paperboard has somewhat stagnated in some parts of the world, global production volume was still over 401 million tons/year, according to statistics from the Food and Agriculture Organization of the United Nations (FAOSTAT 2012). A large share of the production is pigment coated to improve the physical and functional properties of the end-use products. In pigment coating, various types of binders are used to bind the pigment particles together and onto the base paper fibers. The binder has to provide sufficient strength to fulfil end-use requirements, which are usually related to printability and various finishing operations. Insufficient coating strength can lead to problems such as dusting, picking, piling, fold-cracking, and coating deposits on calender rolls. These problems are of significant economic concern to papermakers and printers. Latex is a high-cost binder used extensively in paper coatings, and it has a price dependency on the cost of crude oil. Amid the rising costs of petroleum-based raw materials, the latex price has increased considerably over the last decade. Considering that a continued rising trend in oil prices is to be expected, it is obvious that the binder component in pigment-coated paper products holds substantial savings potential in the future.

When reducing binder levels in pigment coatings below a certain threshold to reduce costs, surface strength suffers and various problems appear that are related to a mechanical failure in the coating layer. While coating strength has been intensively studied [1-4], details of the coating failure mechanisms are still not well understood. Influence of the coating structure and the role of various pigments have been investigated [5-7]. On a macroscopic scale, there is an understanding of how particle shape and specific surface area, for example, set demands on the binder level required for a given surface strength. However, there is uncertainty as to whether the failure in the coating is a cohesive failure of the binder or an adhesive failure at the binder-pigment interface. Investigations [8-13] suggest that polar liquids, such as water from the fountain solution in offset lithography and vegetable-based polar oils in printing inks, decrease the extent of latex bonding on the dispersant-covered pigments. This can potentially lead to problems in printing, such as picking at the later color printing units.

Most of the published work has concentrated on measuring the coating surface strength with techniques mimicking ink film split in printing. While simulating the extensional forces in a printing process, these include contributions not only from coating surface strength but also from the ability of the test liquids to wet the paper surface and penetrate into the coating. Other modes of deformation, such as compression and shear, are also important in inducing coating failure in numerous converting processes. Problems related to con-

verting of pigment coated products, such as fold-cracking, have only recently been studied [14-18].

A further consideration for the surface strength is the distribution of binder in the coating layer. An uneven distribution, such as that caused by binder migration or aggregation, will lead to locally reduced coating strength and a need to use excessive amounts of binder. Binder migration has been studied extensively, but the focus has mostly been on its influence on mottle (i.e., nonuniform ink absorption). Recent increased use of natural binders, such as starch and its derivatives, has raised the question of the role of interactions between the binders for coating strength when using multibinder coating formulations. No comprehensive studies exist in this area.

In general, the current work aims at understanding binder functionality in pigment coatings on molecular and microscopic levels, to increase the efficiency of binder usage. An attempt is made to improve the coating strength by specifically addressing molecular interactions at the binder-pigment surface interface. Three specific objectives were defined: (1) to identify mechanisms of failure when load carrying capacity of a coating is exceeded; (2) to characterize molecular level interactions between binders, dispersants, and coating pigments; and (3) to develop and test modified pigment dispersants to improve the interfacial strength between coating pigments and binders.

MATERIALS AND METHODS

The current work combines several different approaches to address the defined objectives. Herein, only a brief description of the used materials and methods are given. The details can be found in references cited below and listed in the Literature Cited section.

Micromechanical simulations

For modeling of mechanical properties of pigment coating, a triple tier approach was used. First, a cohesive pigment-latex composite model was built with Monte-Carlo particle packing algorithm combined with binder-addition algorithm illustrated in **Fig. 1** and detailed in [19]. The current study investigated monolayers circular particles, but the approach can be extended to the third dimension. Secondly, the microstructure of the numerical model coating layer was characterized for its geometrical (statistical) parameters. These included porosity, anfractuosity (solid phase tortuosity), binder contact lengths, binder-bridge orientations, and pigment particle coordination numbers. Finally, a mesh-free continuum mechanics simulation was used to predict plastic and elastic straining as well as cohesive and adhesive (interfacial) fractures in the model when exposed to extension. Pigment particles were modelled as Hookean elastic materials (Young's modulus of 39 GPa) and latex binder were modelled as nonlinearly elastic material with plastic straining beyond critical strain. Important input parameters to the model are the latex cohesive strength, σ_y, and the latex-particle bond (adhesive) strength, σ_b. These were obtained from tensile tests of pure latex and pull-off tests

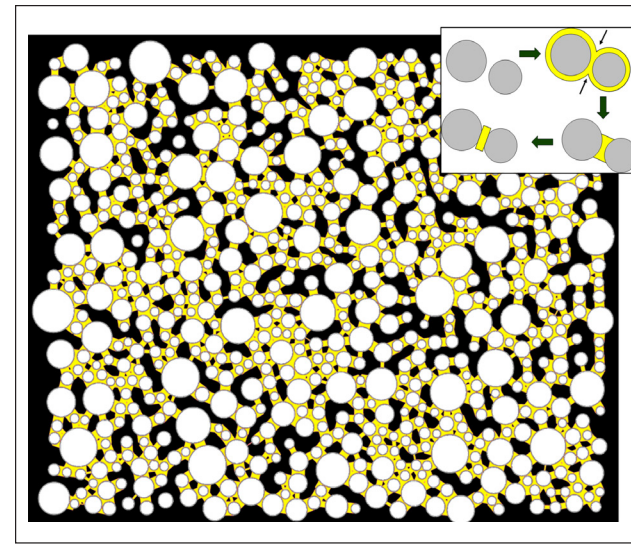

1. Numerical model coating structure with illustration of binder addition algorithm.

of latex bonded to calcite crystal surfaces covered by dispersant.

Output data from the simulations include local stresses and strains in the loading direction, local forces and displacements in the loading direction and along local binder axes, number of connections broken at an interface, number of binder bridges straining plastically, number of binder bridges straining elastically, particle-particle separation distances and global force, displacement, and stress and strain values.

Molecular modeling

Two types of simulations were performed: (1) simulations with a calcite surface, monomeric fragments of latex, and tetrameric fragments of dispersants (**Fig. 2a**) and (2) simulations with a larger, spherical shaped latex particle with tetrameric dispersant fragments (Fig. 2b). For both types of simulations, four simulation systems were built, one for each type of dispersant polymer (**Fig. 3**) included in this work.

In the simulations with a calcite surface the dispersants were described as tetrameric fragments. Eight of those tetrameric dispersant fragments were placed close to the calcite surface using Maestro ver. 9.4 molecular modeling software (Schrödinger LLC; New York, NY, USA). The system was energy minimized and equilibrated, and then a 10-ns molecular dynamics (MD) simulation was performed to allow the fragments to freely find their preferred binding mode on the calcite surface. The calcite surface was kept frozen in space during the simulations. The purpose of these simulations was to create starting structures for the simulations in water.

After the vacuum simulations, the systems were solvated. In addition, styrene-butadiene (SB) latex was added to the simulation system. Latex was described as a group of monomeric latex units: 24 styrene units and 24 butadiene units were placed as a layer above the calcite surface. Finally, the systems were neutralized with randomly positioned Ca^{2+} ions.

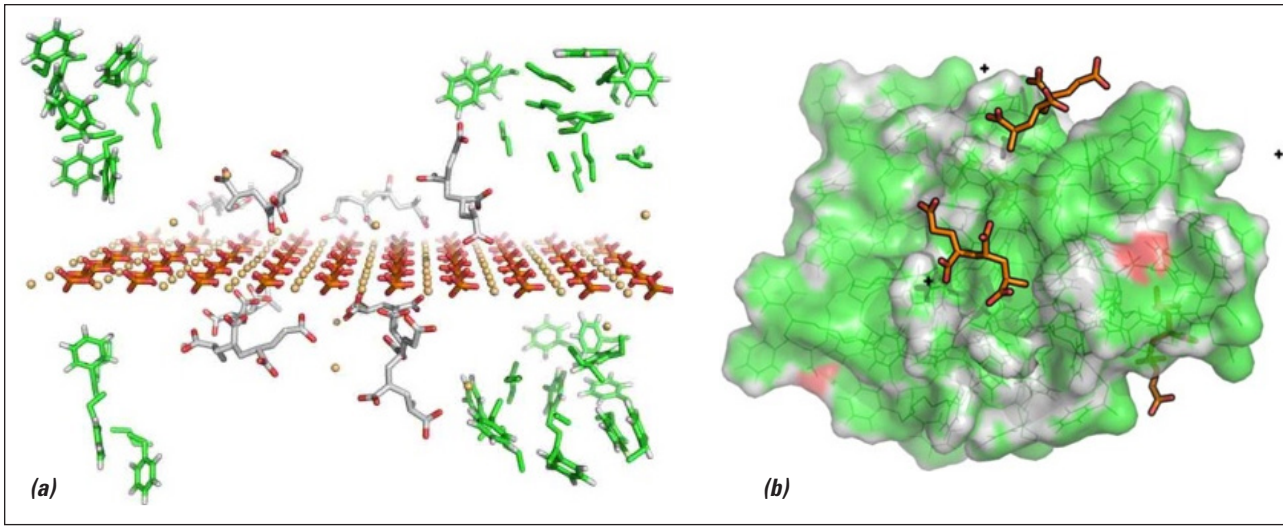

2. Examples of molecular models for (a) calcite (crystal face 1 0 $\bar{1}$ 4) and (b) styrene-butadiene (SB) latex with adsorbed dispersant fragments. Color coding: (a) oxygen = red, calcium = yellow, carbon (polyacrylic acid) = gray, carbon (latex) = green, hydrogen (latex) = white. Color coding: (b) oxygen = red, carbon (polyacrylic acid) = orange, latex surface carbon = green, hydrogen = gray.

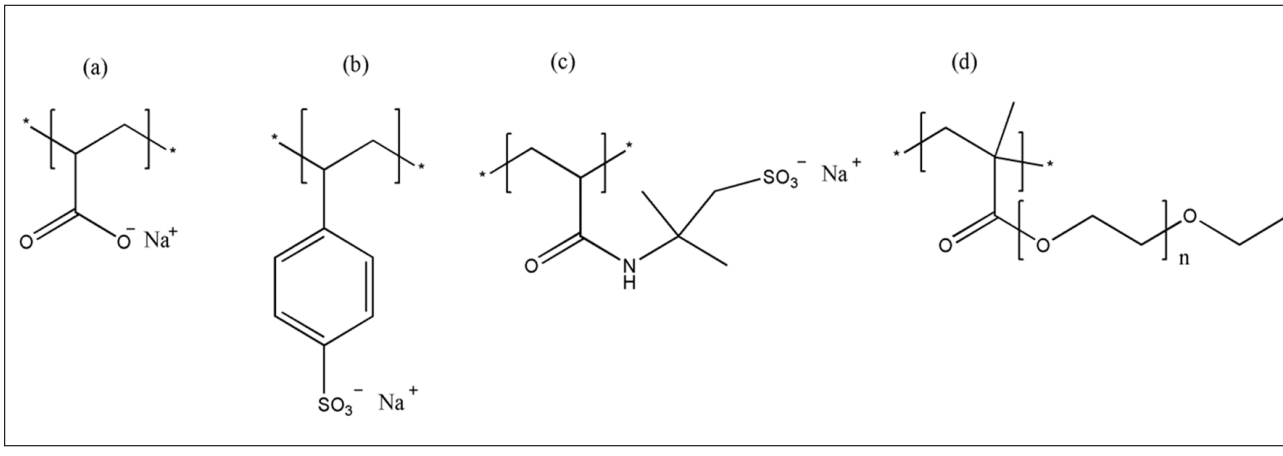

3. Repeating units of the monomers used in dispersant synthesis: (a) polyacrylic acid (AA), (b) poly(styrene sulfonic) acid (SSA), (c) 2-acrylamido-2-methylpropane sulfonic acid (AMPS), and (d) poly(ethylene glycol)ethyl ether methacrylate (mPEG), where n = 3.

After adding the latex fragments and water, the system energy was minimized to remove close contacts. The system was shortly equilibrated and resolvated to fill vacuum bubbles. After this last step, the systems contained approximately 7500 atoms including 2000 water molecules in a 50 Å x 45 Å x 35 Å cubic box. The system was again energy minimized and equilibrated shortly before a production run of 10 ns.

For simulations with a larger piece of latex polymer, the starting coordinates for a spherical shaped latex particle were generated with MD simulations as described in [20]. The SB latex particle contained 72 styrene units, 28 butadiene units, and 6 polyacrylic acid units.

Four tetrameric dispersant fragments were placed on the surface of a latex particle, and the system was solvated with water. Dihedral restraints were applied on the backbone torsions of the fragments to mimic the effect of the calcite by keeping the polymers in the same conformation in which they were binding on the calcite. Then, 5-ns MD simulations were performed for these systems to investigate the interactions of the polymers and latex. The systems contained approximately 17000 atoms including 5000 water molecules in a 55 Å x 60 Å x 55 Å cubic box.

All the simulations were performed with periodic boundary conditions using GROMACS 3.3 software package and GROMOS ffG53a6 [21] force field (University of Gronigen; Gronigen, The Netherlands). The simulations with the calcite surface were performed in constant volume and the simulations with latex particles were performed in constant pressure. The missing parameters for the latex and the polymers were derived in analogy to amino acid parameters in the GROMOS force field. LINCS [22] was used to constrain the bond lengths in the fragments and the SETTLE algorithm [23] was used for the bond lengths and angles of the SPC water mole-

Sample	Composition, mol-%	M_n, g/mol	M_w, g/mol	Polydispersity Index
NaPA*	100	6000	7500	1.25
NaP(AA-r-SSA)*	70-r-30	4500	8700	1.93
NaP(AA-b-SSA)*	70-b-30	7300	11500	1.58
NaP(AA-b-SSA)	80-b-20	8300	11400	1.39
NaP(AA-b-SSA)	90-b-10	7400	9900	1.34
NaP(AA-r-AMPS)	70-r-30	9300	13200	1.42
NaP(AA-r-AMPS)	70-b-30	9700	13400	1.38
NaP(AA-r-AMPS)*	80-r-20	5900	8300	1.40
NaP(AA-b-AMPS)*	80-b-20	8800	11700	1.33
NaP(AA-r-AMPS)	90-r-10	5800	7800	1.33
NaP(AA-b-AMPS)	90-b-10	7600	9900	1.32
NaP(AA-r-AMPS-r-mPEG)*	80-r-15-r-5	7800	11900	1.53

I. Compositions of the synthesized dispersants (r = random copolymer, b = block copolymer). * Chosen for mechanical testing.

cules. The time step was set to 0.002 ps. Temperature was controlled with the Berendsen weak coupling algorithm [24] with coupling constants of 0.1 ps. Coordinates were stored every 10 ps.

Dispersant synthesis

The dispersants were produced by reversible addition-fragmentation chain transfer (RAFT) living free radical copolymerization of acrylic acid (AA) with different functional monomers. This method has been proven effective when modifying polymers with low molecular weight. It also eliminates the drawbacks associated with conventional radical polymerization of AA, such as branching, scissions, and broad molecular weight distribution.

Initially, a series of monodisperse homopolymers of polyacrylic acid with molecular weight (M_w) varying from 2000 g/mol to 12000 g/mol were synthesized using S,S'-Bis(R,R'-dimethyl-R''-acetic acid)-trithiocarbonate RAFT chain transfer agent. Dispersants were further modified through copolymerization of AA with three functional monomers shown in Fig. 3. Each of the dispersants was synthesized in both block (b) and random (r) conformation. Size exclusion chromatography was used to determine the M_w and the polydispersity index (PDI) for the polymers. Polymer structures were verified by nuclear magnetic resonance spectroscopy. **Table I** lists the synthesized copolymer dispersants. A commercial polyacrylate-based dispersant, Sokalan PA30 (BASF AG; Ludwigshafen, Germany), was used a reference dispersant.

Mechanical testing

In mechanical testing, dispersant-free precipitated calcium carbonate OC400 (Imerys Minerals Ltd.; Par, Cornwall, UK; D50 = 0.35 µm, surface area 11 m²/g) and two latexes (styrene butadiene [SB], Dow Deutschland; Rheinmünster, Germany, T_g = 8°C, size = 132 nm, degree of carboxylation 5%, gel content 77% and styrene acrylate [SA] BASF AG, T_g = 20°C, size = 170 nm, degree of carboxylation 4%, gel content 0%) were used. Precipitated calcium carbonate (PCC) was used due to the unavailability of dispersant-free ground calcium carbonate (GCC). The PCC was dispersed at 72% solids content for 20 min, after which either SB latex or SA latex (5, 10, or 15 pph) was added and mixed for 15 min. A constant addition level of dispersant, 0.6 pph, was used throughout, with the exception of results shown in **Fig. 4**. The final solids content was adjusted to 68%, and pH was adjusted by sodium hydroxide if not in the 8–9 range. In **Fig. 5**, predispersed GCC (OC95, Imerys Minerals Ltd.; D50 = 0.55 µm, surface area 12 m²/g) was used.

Samples for the mechanical testing were produced using a custom-built pressure filtration rig with filtration pressure of 0.7 MPa over a 30-nm polycarbonate membrane. The pressure-filtrated rectangular samples, 120 mm long and 80 mm wide, were oven dried at 70°C for 12 h. For testing, the samples were cut into two different sizes: 100 mm² x 10 mm² (thickness 2 mm) for tensile testing and 30 mm² x 5 mm² (thickness 1 mm) for dynamic mechanical thermal analysis (DMTA) testing.

The coating elastic modulus and tensile strength were measured using an Instron 8872 (Instron; Norton, MA, USA) with a deformation rate of 0.5 mm/min at ambient conditions. The tests were performed on rectangular samples because these materials were brittle and could not support further machining to make dog-bone-shaped samples. DMTA was performed using two instruments: Rheometric Scientific DMTA IV at the University of Maine (temperature and frequency sweeps at 0.005% strain) and Triton 2000 DMTA at the University of Bath (temperature sweep in single cantilever bending mode with 0.1% strain amplitude and 1 Hz frequency). Details of the experimental setups can be found in [25-27].

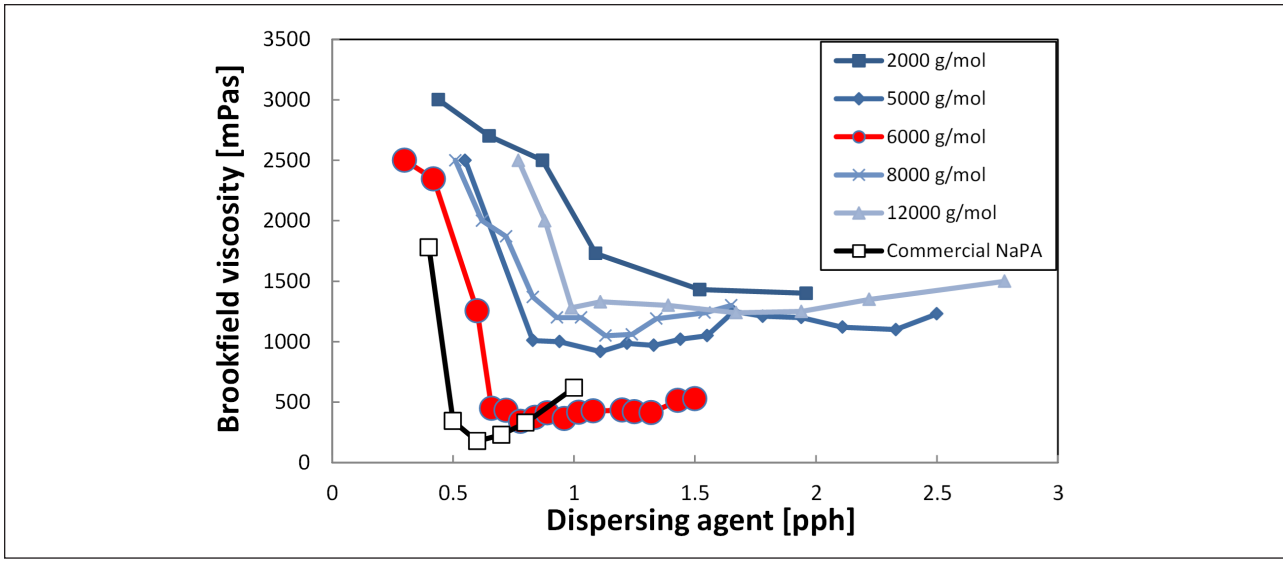

4. Influence of sodium polyacrylate (NaPA) molecular weight on dispersion efficiency. Precipitated calcium carbonate (PCC) suspensions at 72% solids content.

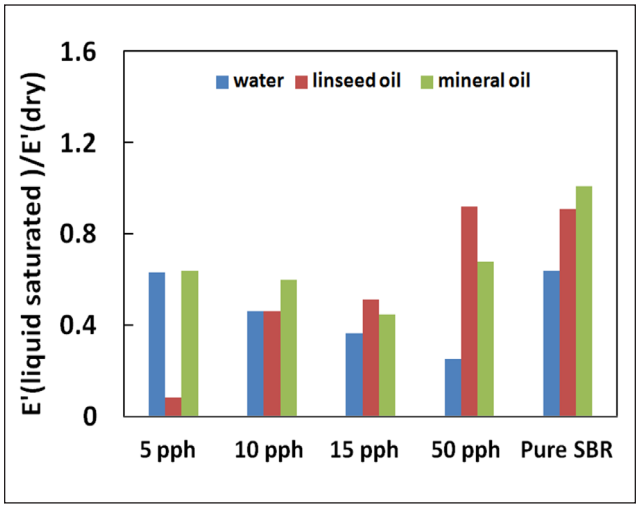

5. Effect of different liquids on the stiffness of predispersed ground calcium carbonate–styrene-butadiene (GCC–SB) latex coatings at room temperature and at 1 Hz.

Surface strength measurement

The surface strength of coatings as applied on paper was measured with dry and wet pick tests. Paper samples were prepared by coating woodfree base paper (70 g/m²) with PCC dispersed with the synthesized dispersants and combined with either SB latex or SA latex. The coatings were carried out with a table top rod coater (K Control Coater, RK Print Coat Instruments Ltd.; Litlington, UK) with a target coat weight of 15 g/m². The coated papers were dried with an infrared drier and calendered with a laboratory calender (DT Paper Science Oy AB; Turku, Finland; 5 nips, 23°C, 30 kN/m).

The dry pick test was performed with an IGT AC2 laboratory printability tester according to ISO 3783 "Paper and board—determination of resistance to picking—accelerated speed method using the IGT-type tester (electric model)." The wet pick test was carried out similarly to the standard dry pick test, with accelerating speed, but with prewetting of the paper surface with about 0.860 g/m² water applied with a smooth print cylinder. The delay between the prewetting and the surface strength testing was kept constant at 10 s. Four parallel tests for both dry pick and wet pick were done. Details of the method are in [28].

Viscosity measurement

Viscosities of the pigment dispersions at 72% solids content were measured at 24°C with a Brookfield viscometer (spindle 4, 100 rpm) and with a Paar Physica MCR 300 rheometer (Anton Paar GmBH; Graz, Austria) with CC27 concentric cylinder geometry.

RESULTS

Numerous micromechanical simulations were carried out to identify coating layer failure modes and related critical microstructural parameters controlling coating strength. Previous results are summarized in [29]. That work also proposes an improved mixtures model to predict Young's modulus of porous coating based on microstructural considerations such as particle shape, anfractuosity, and linear porosity perpendicular to the direction of deformation. Of special interest in the current work was understanding how paper coatings fail if their mechanical loading capacity is exceeded. A ductile cohesive failure within the binder followed by high levels of plastic straining indicate that the binder material is used to its fullest mechanical potential. In contrast, adhesive failures at pigment-binder interfaces can be expected to lead to poor mechanical properties of the pigment coating composite.

Figure 6 summarizes results from several simulations in which extensional deformation was applied to numerical

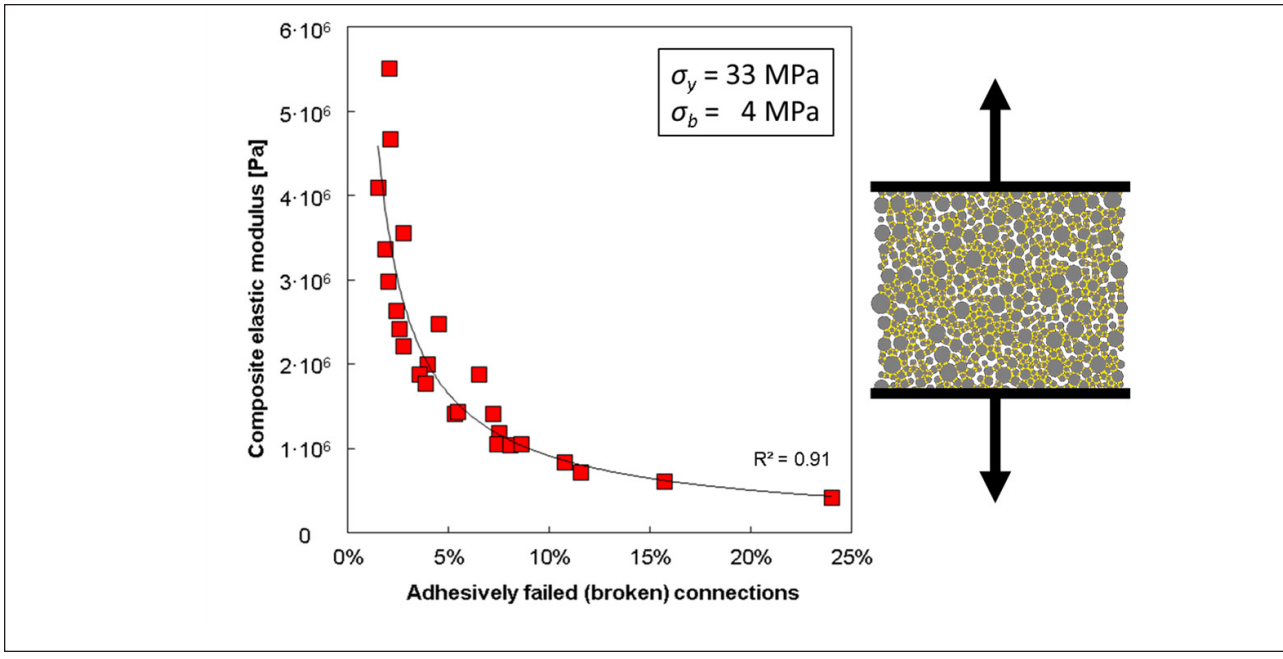

6. Predicted residual elastic modulus versus percentage of adhesive failures in model coating structures during forced extension. The binder-pigment surface adhesive failure stress σ_y is 33 MPa and the cohesive binder strength σ_b is 4 MPa.

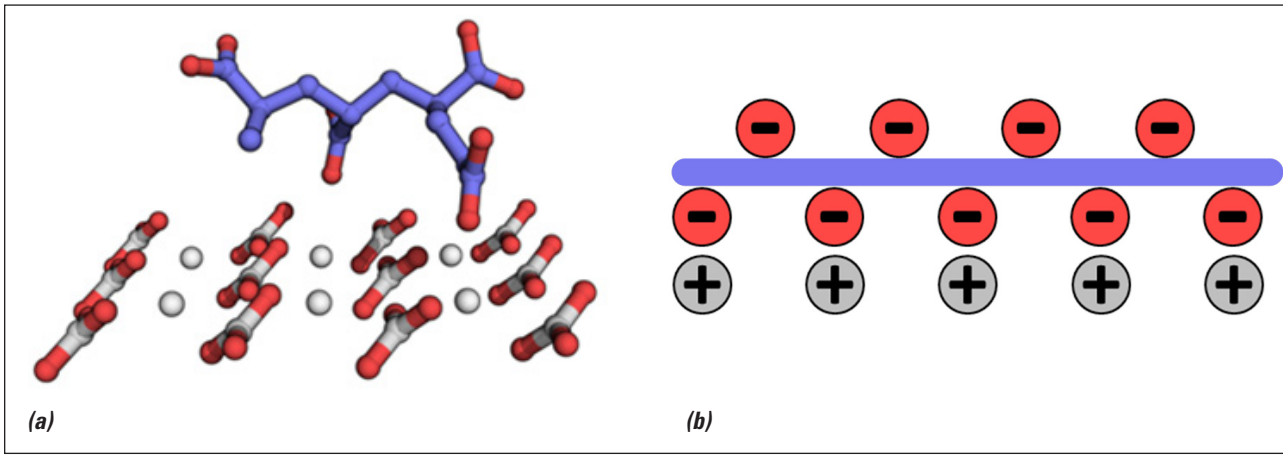

7. (a) Snapshot structure of molecular dynamics (MD) simulation of polyacrylate binding to calcite surface, and (b) cartoon illustration of polyacrylate binding on calcite. Color coding: blue = polyacrylate backbone, red = oxygen, gray = calcite calcium ion.

model coating layers. As the coating is being extended, through forced constant motion of the top and bottom boundary particles, the predicted residual elastic modulus is calculated in time, and failure modes (cohesive/adhesive) are recorded for each failed pigment-pigment pair connected by binder. Details of the simulation approach are reported in [19]. It is apparent that, based on the simulations, the coating rapidly loses its strength after a small percentage of pigment connections have failed adhesively. This suggests that to improve or maintain the coating strength, it is crucial to ensure adequate adhesion between pigment surfaces and the used binder. Husband et al. and Lazarus et al. [11,12] have shown loss of pigment coating strength due to polar liquids and propose the loss of pigment-binder adhesion as a mechanism.

At the molecular level, the pigment-binder interfacial behavior is influenced by dispersant, which fully covers the pigment surfaces, especially in the case of calcium carbonate. The purpose of dispersants is to provide electrostatic and osmotic pressure-driven repulsion between the pigment particles to counteract their tendency to agglomerate due to van der Waals forces. Typical polyacrylate-based dispersants in paper coating are highly charged and hygroscopic. This is illustrated in **Fig. 7**, which shows the polyacrylate binding conformation on a calcite surface as predicted by MD simulation. Here, every other acid group binds to the surface, alternating with every other acid group that points outward to solvent or binder, if present. This hydrophilic surface leads to effective pigment dispersion but does not favor binding to a

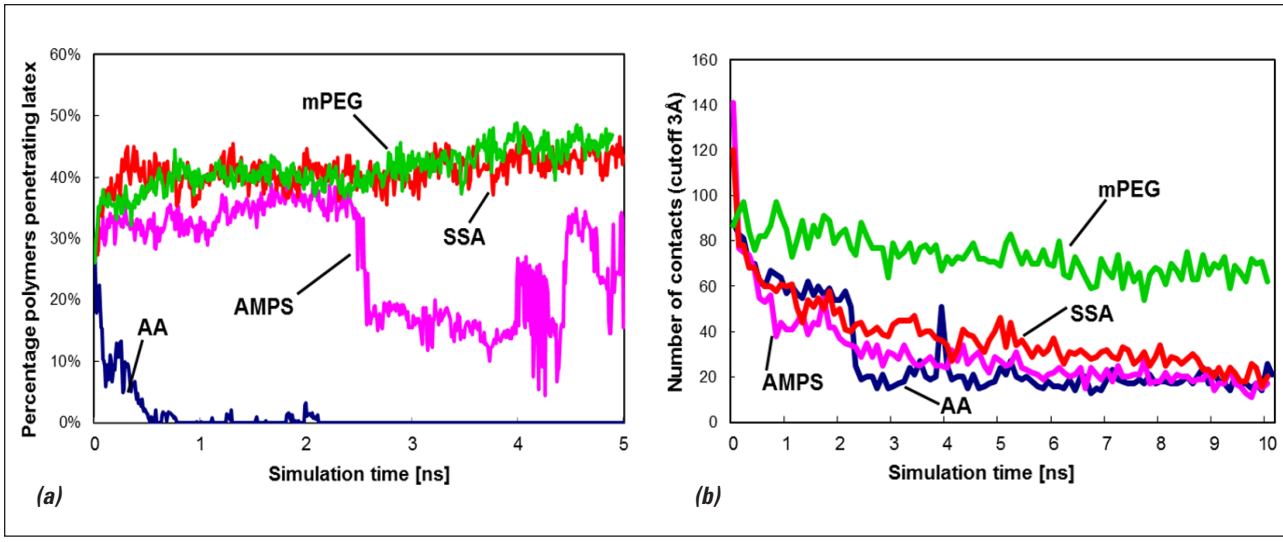

8. (a) Dispersant-calcite interaction; number of contacts between dispersant polymer and calcite surface (cutoff distance = 3Å) and (b) dispersant-latex interaction; the percentage of the polymers penetrating into the latex surface.

hydrophobic latex backbone. To provide stability in dispersion, latexes used in paper coating are typically carboxylated, which also promotes spreading of latex on pigment surfaces [30]. However, the combined effect of latex carboxylation and the hydrophilicity of the sodium polyacrylate (NaPA)–covered pigment surface creates an interface that can be sensitive to humidity and polar liquids, such as fountain solution and vegetable oils used in sheet-fed offset lithography printing. This can be hypothesized to have a detrimental effect on the effective coating wet strength. To test this hypothesis, and potentially increase the coating layer wet strength, bifunctional dispersants were synthesized and tested. The chemistries for the dispersants were chosen to provide adequate dispersing effect for pigments in suspension and improve the binding between pigment surfaces and the latex binder in the presence of polar liquids.

Initially, the role of M_w on the dispersing effect of NaPA was investigated. Figure 4 shows that for monodisperse NaPA homopolymer, the lowest viscosity and lowest dosage is achieved with M_n = 6000 g/mol. These values are similar to those values of the commercial NaPA dispersant, which indicates that the dispersant synthesis was successful. In continuation, the target molecular weight of M_n = 6000 g/mol was used. An advantage of the RAFT polymerization is the accurate control of M_w. Commercial dispersants typically have much wider M_w distributions than those synthesized by the RAFT technique.

The NaPA homopolymer dispersant was modified through copolymerization with three functional groups shown in Fig. 3. In parallel, molecular-level interactions between the functional groups, coating pigment surface, and latex were studied with MD simulations. The molecular simulations predict that 2-acylamido-2-methylpropanesulfonic acid (AMPS) and poly(styrene sulfonic) acid specific surface area (SSA) functional groups bind onto calcite surfaces using their negatively charged sulfate groups. NH protons of AMPS appear also to participate in the binding. For poly(ethylene glycol)ethyl ether methacrylate (mPEG), the carbonyl oxygen and the side-chain oxygen contribute to the binding. The modified dispersant and calcite surface interaction was quantified by calculating the number of contacts (distance d < 3Å) between a dispersant polymer and the calcite surface during an MD simulation. As **Fig. 8a** shows, mPEG-modified dispersant seems to behave differently by having higher affinity to the calcite surface than the other dispersant polymers. The results suggest that positioning of oxygen in mPEG side chain is suitable for creating stable electrostatic contacts with calcium ions on calcite.

Dispersant tetramer interaction with SB latex was simulated similarly. Fig. 8b shows how the NaPA dispersant (labeled AA) without any functional groups is predicted to have minimal affinity to the latex polymer, whereas SSA and mPEG functional groups promote interaction. The hydrophobic backbone of mPEG binds to latex and hydrophilic side chains direct themselves mostly to the solvent, as illustrated in **Fig. 9a**. SSA tetramer embeds itself deeply into the latex, leaving only the charged sulfate groups out in the solvent (Fig. 9b). The main attractive interaction is between SSA phenyl moieties and phenyl groups of the latex.

Preliminary screening of the synthesized polymers in Table I was done by eliminating those not having sufficient dispersing effect or leading to high viscosity of PCC dispersion. The dispersants highlighted and indicated with asterisk in Table I were further tested for their dispersing efficiency and the ability to increase the coating mechanical strength in the presence of polar liquids. All the dispersants had an AA backbone to which the various functional groups were copolymerized either as random (r) or block (b) copolymers using molecular fractions shown in column two in Table I.

Shear viscosities of pigment suspensions dispersed by the

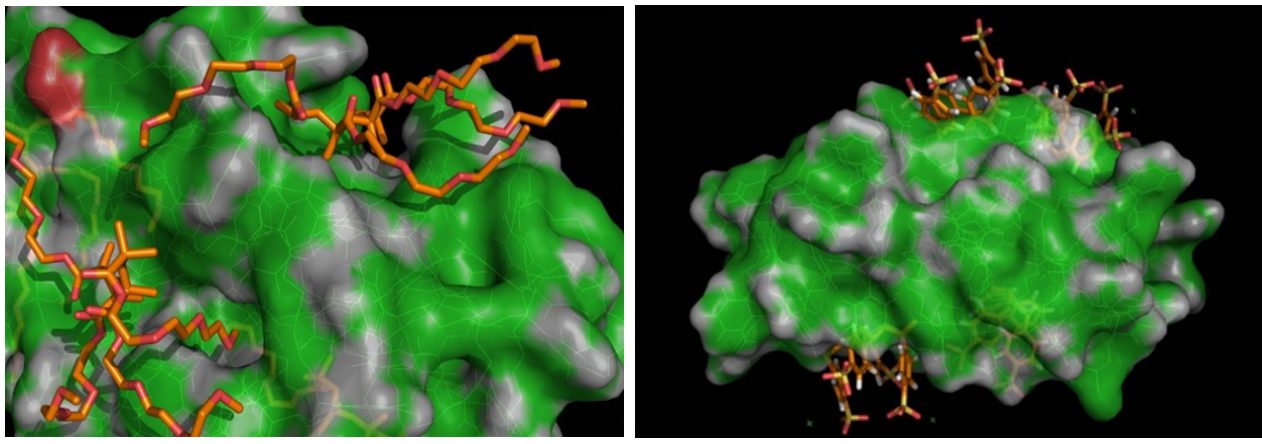

9. (a) mPEG and (b) SSA tetramer interactions with the SB latex. Color coding (dispersant): carbon = orange, oxygen = red, hydrogen = white, sulfur = yellow. Color coding (latex surface): carbon = green, hydrogen = gray.

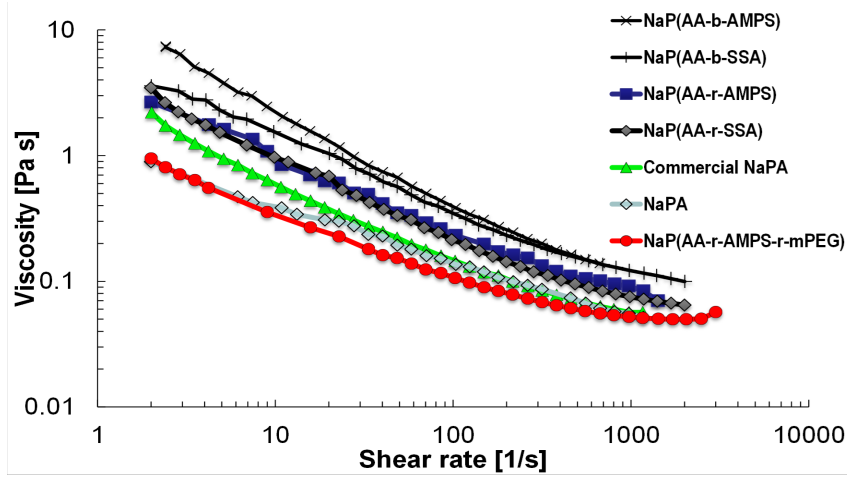

10. Low-shear viscosity of PCC pigment suspensions (72% solids content) dispersed with 0.6 pph of the synthesized dispersants. Dispersant details are in Table I.

synthesized polymers highlighted in Table I are in **Fig. 10**. While the dispersing effect in this case was not extensively investigated and the rheological characterization is limited to relatively low shear rates, it is clear that the polymers do create stable suspensions. The use of the dispersant incorporating both the MPEG and AMPS moieties as random copolymer results in the lowest viscosities, somewhat lower than both the commercial and NaPA synthesized here. Suspensions dispersed with block copolymers, and with SSA and AMPS functional groups, led to the highest viscosities.

Of note, in these tests a constant addition level of 0.6 pph dispersant was used. Optimizing the addition level for each dispersant might lead to lower viscosities. Excessive amounts of a dispersant leads to an increase in viscosity due to the increased electrolyte concentration from nonadsorbed polymer, which screens the electrostatic repulsion between particles. Furthermore, due to the differences in the dispersant chemistry and the M_w, the polymers have different lengths, which has been shown to influence polymer adsorption and conformation on pigment surfaces with further effects on the dispersing effect.

The influence of the modified dispersants on the mechanical properties of coatings prepared with them was measured with tensile testing, DMTA, and the standard dry and a modified IGT wet pick test. **Figure 11** summarizes the results from tensile testing of pressure-filtrated coating samples for SB latex and SA latex addition levels of 5, 10, and 15 pph. The intrinsic latex tensile strength, determined by T_g, gel content and other latex parameters, influences the mechanical properties whereby the SA latex-based coatings have here higher tensile strength than SB latex-based ones. The AMPS and SSA-based dispersants show low elastic modulus and tensile strength for both latexes and at all latex addition levels. Dispersants modified with mPEG functional group give rise to as high as, and in some

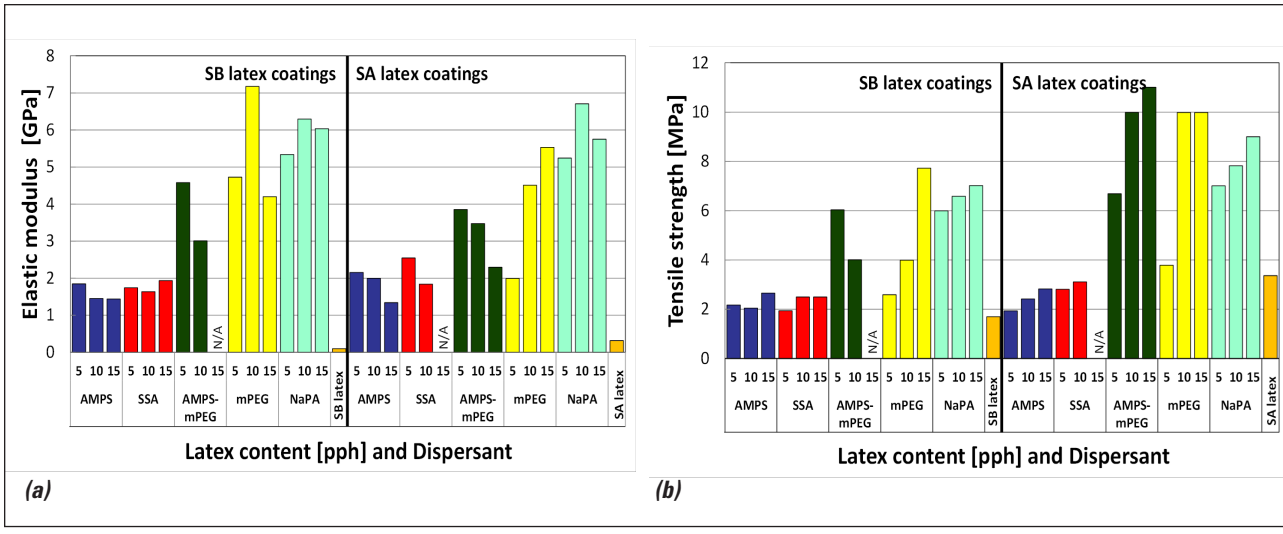

11. (a) Elastic modulus and (b) tensile strength of different PCC-based coatings measured with tensile tests of pressure-filtrated samples.

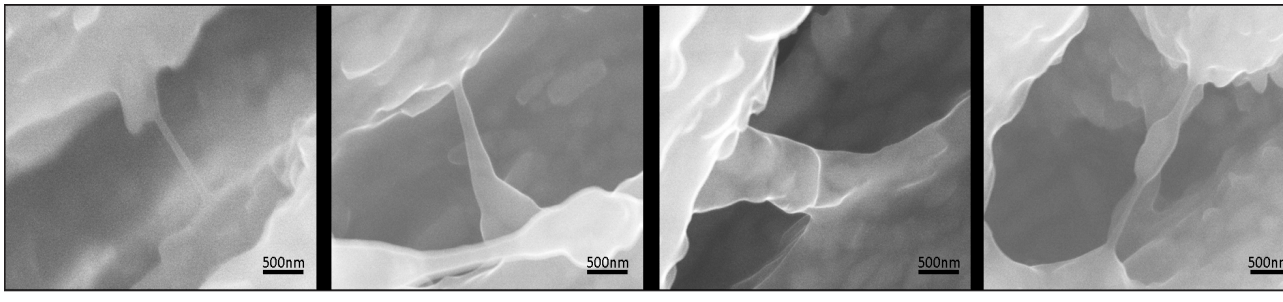

12. Latex bridges in cracks in the coating dispersed by mPEG-modified dispersant.

cases even higher, tensile strength when compared to pure NaPA. Some support for this can be found in scanning electron microscope images taken from the samples after mechanical testing. For samples dispersed with mPEG-modified dispersant, numerous fibrillar latex bridges can be seen in the cracks induced by the tensile deformation indicating high latex-pigment adhesion (**Fig. 12**). The number of such latex bridges was clearly lower in all the other samples. The sample porosities were measured using a Pascal 140-440 porosimeter (Thermo Fischer Scientific; Waltham, MA, USA) but no correlation to the observed differences in mechanical properties at constant latex addition level could be seen.

The influence of liquids on the mechanical properties was investigated with DMTA. Figure 5 shows the loss in the elastic modulus when samples consisting of commercial predispersed GCC and SB latex are exposed to water, linseed oil, and mineral oil. The observed weakening can be caused either by pigment-binder interface adhesion failure or by plasticization of the bulk polymeric binder by the liquids. Separation of the two mechanisms, which most probably both play a role, was not possible herein. Interestingly, the elastic modulus increases when linseed oil addition level is increased from 5 pph to 50 pph. This could be due to polymer entanglement or cross-linking caused by autoxidation of the

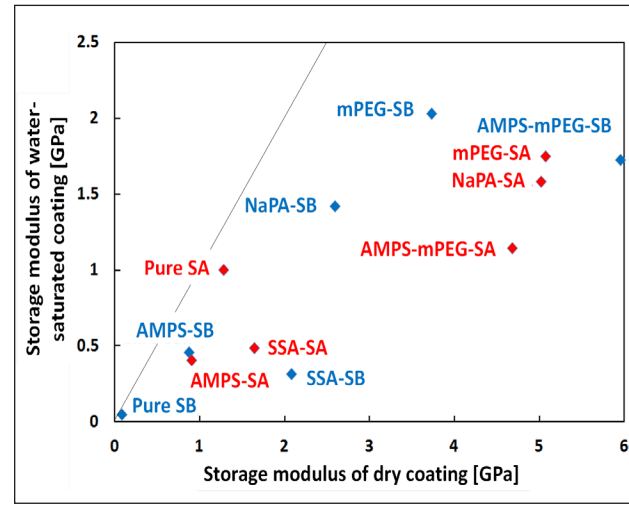

13. Comparison of the storage modulus of PCC-10 pph latex coatings at room temperature as dry and after water saturation.

unsaturated fatty acid components in linseed oil [31].

Figure 13 compares the storage modulus of PCC–10 pph latex coatings at room temperature as dry and after water saturation (immersion in deionized water for 24 h); both SB latex and SA latex were used. The SA latex coatings show

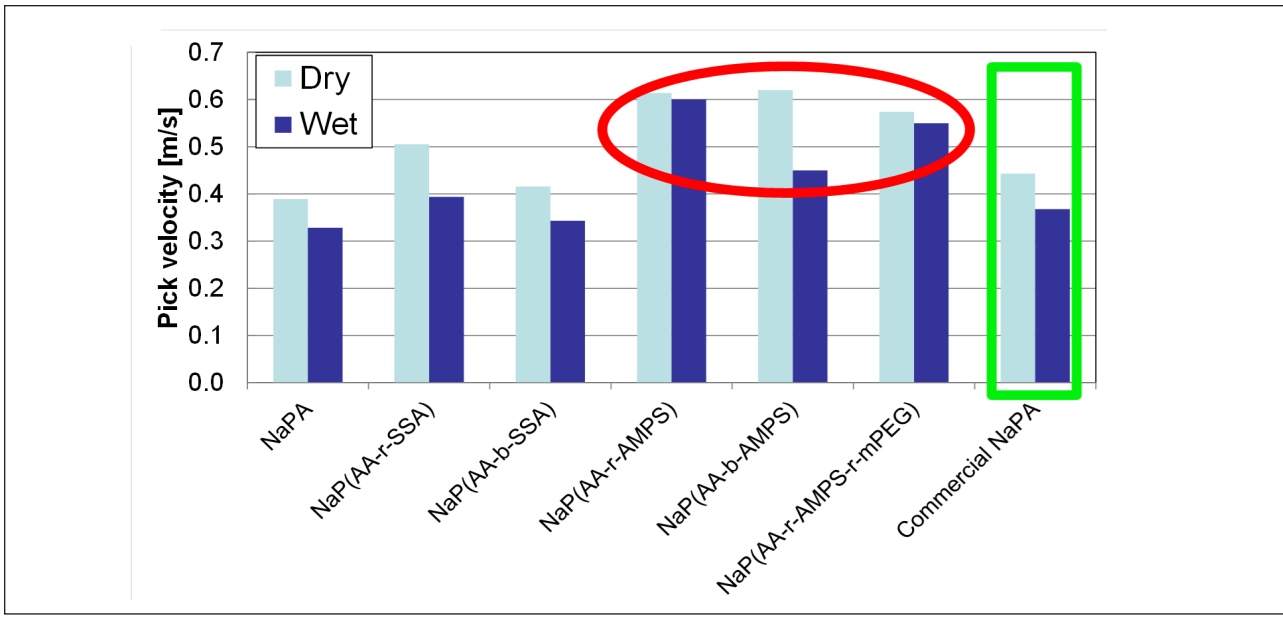

14. Surface pick strength: PCC + 10 pph SB latex (Tg = 8°C, d = 132 nm), fine paper base. Dry pick = standard IGT dry pick test, wet pick = the same with prewetting.

relatively higher stiffness than SB latex coatings due to the high T_g of SA latex compared to SB latex. Functionalizing a dispersant with MPEG groups seems to enhance the coating stiffness by improving the compatibility with the latexes and also improving the interfacial resistance to attack by water. The interpretation of the results from DMTA is complicated by secondary effects (e.g., the porosity of the samples changes when changing the dispersant). This also influences the accessibility of the pigment-binder interfaces by absorbing liquids. A more thorough analysis and details of the DMTA measurements are in [32].

Finally, the surface strength of the on-paper-coated samples was tested with dry pick and wet pick tests. The results in **Fig. 14** show somewhat higher pick resistance for some of the modified dispersants when compared to a commercial NaPA dispersant. Two polymers, NaP(AA-r-AMPS) 80-20 and NaP(AA-r-AMPS-r-mPEG) 80-15-5, appear to maintain the surface strength best when tested after prewetting of the paper surface.

CONCLUSIONS

Through a combination of various experimental and simulation approaches, this work attempted to better understand the microscopic and molecular level interactions between latex binder and coating pigments covered by dispersants. The increased understanding can potentially provide solutions to improve surface strength of pigment-coated paper and board and lead to higher cost efficiency in production.

Micromechanical computer simulations of model coating structures suggest that at low latex concentrations the strength properties are determined by adhesion at the pigment-dispersant-binder interfaces. This, together with previously published data, led to the hypothesis that if coating strength in the presence of polar liquids is reduced by weakening of bonding at interfaces, it can be counteracted by use of bifunctional dispersants that disperse pigments in wet coating slurry and also improve binder-pigment adhesion in a dry coating layer.

Several new pigment dispersing agents were synthesized and tested for their dispersing efficiency. The synthesis of the dispersing agents was successful; all of them were able to disperse pigments. While some of the dispersants showed lower pigment suspension viscosity when compared to pure NaPA dispersant, further studies are needed to clarify this. For example, adsorption isotherms are needed to better understand the pigment-dispersant interaction in wet state. Potentially improved dispersion efficiency through dispersant modification can provide a way to reduce viscosities at constant solids content, or enable use of higher solids content in pigment coating colors.

In parallel to the experimental work, MD simulations were used to investigate interactions of the functional groups used in the dispersants with pigment (calcite) and latex. The MD modeling showed differences between the polymer types in their binding and affinities on the calcite and latex. Modeling also suggested that functional groups in mPEG and SSA monomers are least sensitive to water and could thereby potentially improve interfacial adhesion in aqueous environment. Carboxylation of latex appeared to improve the wetting (spreading) of latex on dispersant-covered pigment surfaces.

Some of the functionalized dispersants showed as high or higher dry and wet strength in mechanical testing and in DMTA of pressure-filtrated pigment-latex samples when compared to dispersants based on pure polyacrylate chemistry. For the SB latex, the storage modulus of the samples prepared with the mPEG-modified dispersant was higher than that of

samples dispersed with NaPA, both in dry state and after water saturation. For laboratory-scale coated paper sheets, similar results were seen in IGT pick test, both with and without prewetting. Also, mPEG monomer seemed most promising as a modifier for the NaPA-backbone dispersant. However, use of AMPS monomer together with mPEG appeared to provide further improvements. The synthesized dispersant functionality seemed to be somewhat sensitive to small changes in the relative amounts of functional monomers used. This, combined with the need to find an optimal dosage for each dispersant, makes optimization of the dispersant chemistry time-consuming. However, based on the results, a conclusion is that random copolymers appear to perform better than block copolymers.

The mechanism by which the modified dispersants improve the wet strength is somewhat uncertain. The MD simulations suggest better interaction between the copolymerized functional groups and the latex binder; however, because some of the used monomers reduce the dispersant hydrophilicity, reduced water absorption by the coating during prewet-

ABOUT THE AUTHORS

Because the binder is the highest-cost component in pigment coatings, we wanted to look for solutions to improve the coating strength without modifying the binder itself. Previous research by others had shown, in macroscopic scale, the sensitivity of pigment-binder interface to polar liquids. We wanted to investigate the topic hierarchically from molecular to microscopic to macroscopic scale, as well as propose solutions to overcome the problem.

In general, coordination of the multitier approach, molecular dynamics and micromechanical simulations, synthesis of novel dispersants, and their testing within the given project timeframe was challenging. Maximization of communication between the research groups and frequent meetings with the industrial partners helped to focus the project in practice. We found that some of the synthesized dispersants showed considerably better dispersing effect, measured as coating suspension viscosity, than commercially available ones.

The increased understanding of molecular-level interfacial phenomena of paper coatings can provide solutions to improve surface strength of pigment coated paper and board, and lead to better production cost efficiency. Specifically, bifunctional dispersants can potentially improve wet strength of paper coatings. The next step is to upscale the most promising dispersant chemistries and test them in larger scale.

Toivakka is a professor, Alam is an adjunct professor, Touaiti is a postdoctoral researcher, and Pahlevan is a doctoral student at the Laboratory of Paper Coating and Converting, and Center for Functional Materials, Åbo Akademi University, Turku, Finland. Wilen is a professor, Nilsson is a master's student, and Ahokas is a postdoctoral researcher at the Laboratory of Polymer Technology, and Center for Functional Materials, Åbo Akademi University, Turku, Finland. Knuutinen is a professor and A. Oravilahti is a doctoral student at the Department of Chemistry, University of Jyväskylä, Jyväskylä, Finland. T. Oravilahti is a pharmacoeconomist at the Finnish Medicines Agency, Kuopio, Finland. Email Toivakka at Martti.Toivakka@abo.fi.


Toivakka


Wilen


Alam


Nilsson


Pahlevan


Ahokas


Knuutinen


A. Oravilahti


Touaiti


T. Oravilahti

ting can also partially explain the observed improvements in wet pick resistance. This, of course, should be seen as a potential way to reduce the picking problem in an industrial printing process, if it does not lead to other problems, such as mottle. Finally, the results from the current work should be further explored and verified in large-scale studies. **TJ**

ACKNOWLEDGEMENTS

The authors gratefully acknowledge the financial support from the Finnish National Agency for Technology and Innovation (TEKES), grants 40074/07 and 40187/09, and the industrial partners of the OptiBind-consortium. The authors thank the University of Maine and the University of Bath for giving access to DMTA.

LITERATURE CITED

1. Prall, K.M., "Viscoelastic behavior of pigmented latex coating films," Ph.D. thesis, University of Maine, Orono, ME, 2006.
2. Toivakka, M. and Bousfield, D.W., "Modeling of coating layer mechanical properties," *Adv. Coat. Fundam. Symp.*, TAPPI PRESS, Atlanta, GA, USA, 2001.
3. Rättö, P., *J. Pulp Pap. Sci.* 30(12): 335(2004).
4. Husband, J.C., Preston, J.S., and Blair, D., "New insight into the printing strength of calcium carbonate coatings," *23rd PTS Coating Symp.*, Papiertechnische Stiftung, Munich, 2007.
5. Parpaillon, M., Engström, G., Pettersson, I., et al., *J. Appl. Polym. Sci.* 30(2): 581(1985).
6. Husband, J.C., Preston, J.S., Gate, L.F., et al., *TAPPI J.* 5(12): 3(2006).
7. Husband, J.C., Preston, J.S., Gate, L.F., et al., *TAPPI J.* 6(12): 10(2007).
8. Reinius, H., Pajari, H., Tahkola, K., et al., "Knowledge of the interactions between fountain solution and coating provides ways to improve printed paper quality," *21st PTS Coating Symp.,* Papiertechnische Stiftung, Munich, 2003.
9. Preston, J.S., Husband, J.C., Norouzi, N., et al., "Printing strength and analysis of the distribution of model fountain solution in kaolin and calcium carbonate coatings," *PaperCon*, TAPPI PRESS, Atlanta, 2008.
10. Husband, J.C., Gate, L.F., Preston, J.S., et al., "The effect of water and oils on the strength of latex bound coating during offset printing," *Prepr. - Int. Pap. Coat. Chem. Symp., 7th*, Pulp and Paper Technical Association of Canada, Montreal, 2009.
11. Husband, J.C., Gate, L.F., Preston, J.S., et al., *J. Adhes. Sci. Technol.* 224(3): 493(2010).
12. Lazarus, E., Salminen, P., Alam, P., et al., "Fundamental mechanisms for dry and wet coating strength," *29th PTS Coating Symp.*, Papiertechnische Stiftung, Munich, 2011.
13. Lazarus, E., Alam, P., Salminen, P., et al., "On the mechanisms of wet and dry strength of paper coatings: part 1—experimental studies," *PaperCon*, TAPPI PRESS, Atlanta, 2012.
14. Salminen, P., Carlsson, R., Sandås, S., et al., "Combined modeling and experimental studies to optimize the balance between fold crack resistance and stiffness for multilayered paper coatings: part 1—introduction and modeling studies," *Coat. Graphic Arts Conf. Trade Fair*, TAPPI PRESS, Atlanta, 2008.
15. Salminen, P., Carlsson, R., Sandås, S., et al., "Combined modeling and experimental studies to optimize the balance between fold crack resistance and stiffness for multilayered paper coatings: part 2—pilot coater experimental studies," *Coat. Graphic Arts Conf. Trade Fair*, TAPPI PRESS, Atlanta, 2008.
16. Yang, A., Xie, Y., and Renjung, W. "From theory to practice: improving the fold crack resistance of industrially produced triple coated paper," *PaperCon*, TAPPI PRESS, Atlanta, 2011, p. 1845.
17. Rättö, P., Hornatowska, J., Changhong, X., et al., *Nord. Pulp Pap. Res. J.*, 26(4): 485(2011).
18. Alam, P., Toivakka, M., Carlsson, R., et al., *J. Compos. Mater.* 43(11): 1265(2009).
19. Alam, P. and Toivakka, M., *Key Eng. Mater.* 462–463: 24(2011).
20. Ylikantola, A., Linnanto, J., Knuutinen, J., et al., *J. Mol. Struct.: THEOCHEM* 953(1-3): 123(2010).
21. Oostenbrink, C., Villa, A., Mark, A.E., et al., *J. Comput. Chem.* 25(13): 1656(2004).
22. Hess, B., Bekker, H., Berendsen, H.J.C., et al., *J. Comput. Chem.* 18(12): 1463(1997).
23. Miyamoto, S. and Kollman, P.A., *J. Comput. Chem.* 13(8): 952(1992).
24. Berendsen, H.J.C., Postma, J.P.M., van Gunsteren, W.F., et al., *J. Chem. Phys*. 81(8): 3684(1984).
25. Touultiaiti, F., Alam. P., Toivakka, M., et al., *J. Mater. Sci. Eng. A* 527(9): 2363(2010).
26. Touaiti, F., Alam, P., Toivakka, M., et al., *Mech. Mater.* 49: 1(2012).
27. Touaiti, F., Pahlevan, M., Nilsson, R., et al, *Prog. Org. Coat.* 76(1): 101(2013).
28. Nilsson, R., "Bestämning av våtnappningsmotstånd hos bestruket papper med IGT-AC2" (in Swedish), Bachelor's thesis, Abo Akademi University, Turku, Finland, 2013.
29. Alam, P., *Mech. Res. Commun.* 37(4): 389(2010).
30. Granier, V., Sartre, A., and Joanicot, M., *J. Adhes.* 42(4): 255(1993).
31. Lazzari, M. and Chiantore, O., *Polym. Degrad. Stab.* 65(2): 303(1999).
32. Touaiti, F., Alam, P., Nilsson, R., et al., *Prog. Org. Coat.* 76(2–3): 439(2013).